0273-2289/1559-0291 (Online)/07/136/0141/$30.00

# Mathematical Modeling of Flow and Kinetics in a Reactor for Dilute-Acid Hydrolysis of Cellulose Particles

## *A Mixture Flow Approach*

**Sima Zahrai**[1,*] **and Gunilla Wikström**[2]

*[1]Etek, Etanolteknik AB, Box 50, SE-89121 Örnsköldsvik, Sweden E-mail: sima.zahrai@gmail.com; and [2]Department of Computing Science, Umeå University, 901 87 Umeå, Sweden E-mail: wikstrom@cs.umu.se*

**Received September 12, 2005; Revised February 11, 2006; Accepted February 15, 2006**

## Abstract

A mathematical model to simulate the dilute-acid hydrolysis process of cellulose particles is presented. In this model, the mass is treated as a mixture of different components. A test case is considered for which transport equations for components are developed and solved together with the momentum equation for the fluid flow. To solve the model equations, a commercially available flow solver was used. All input data were taken from previously published works. For the small static mixer considered as test geometry, the result, in terms of the conversion of the cellulose particles, was reasonable. With input parameters that are relevant to a plant-size reactor, the model can be used to predict the conversion of both cellulose and hemicellulose particles.

**Index Entries:** Dilute-acid hydrolysis; computational fluid dynamics; mixture model; mass fractions; viscosity.

## Introduction

The interest in alternative renewable energy sources has been on the rise owing to worldwide awareness of environmental issues associated with the use of fossil fuels. Using bioethanol as a form of liquid fuel benefits the environment by reducing greenhouse effects and harmful gas emis-

---

[*] Author to whom all correspondence and reprint requests should be addressed.

sions. Bioethanol can be produced using wood as biomass. The process involves saccharification of the cellulose and hemicellulose fractions. The sugar can then be fermented to ethanol using ordinary baker's yeast. The remaining solid residue consists mainly of lignin, which can be burned to produce heat (*see* refs. *1* and *2*).

The National Renewable Energy Laboratory built a pilot plant to convert lignocellulosic feedstock into ethanol *(3)*. In this plant, which began operating in 1995, the biomass is pretreated by dilute sulfuric acid and water in a flow-through reactor. By the end of 2004, a pilot plant of a much larger scale, based in Örnsköldsvik in Sweden, began operating flow-through reactors.

During hydrolysis in a flow-through reactor, the degree of the conversion is affected by a number of factors, such as the concentration of dilute acid, the material properties of the biomass, the flow of the biomass and that of the injected acid, and the design of the screw conveyer that transports the mass. Optimization of these parameters could be facilitated considerably if a mathematical model was used to simulate the process.

Such a mathematical model will result in a complex system of equations to be solved for both the flow and the chemical reactions. In the earlier related mathematical modeling, either the flow equations are simplified or the chemical reactions are not accounted for, in order to focus on the flow effects and design issues instead. For example, in studies by Lee et al. *(4)* and Pettersson et al. *(5)*, simplified equations were used, whereas in studies by Wan and Hanley *(6,7)*, chemical reactions remain unaccounted for.

In this article, we propose a model in which both chemical reactions and flow are considered. To reduce computational efforts, we tested the model in a small static mixer, which corresponds in size to the space between two consecutive screw blades in a large-scale reactor. In this test, we simulate the conversion of cellulose particles. Nevertheless, the procedure may easily be applied to other geometries and types of particles.

## Mathematical Modeling

In the dilute-acid hydrolysis of cellulose particles, sulfuric acid may be used as a catalyst to convert cellulose into sugar. The sugar is then degraded into decomposed material. Hence, there are a number of different species within a reactor in which the hydrolysis process takes place. In a continuous-flow reactor, the concentration of each species is governed by chemical reaction and/or flow convection and is mathematically described by a transport equation. Here, we describe the flow field as a multicomponent single-phase flow and begin by defining the following quantities.

### *Definitions*

Mass-average density of fluid component i in the mixture, i.e., the mass of the component per unit volume, is denoted by $\tilde{g}_i$. Average density is calculated from Eq. 1, in which A, B, C . . . is the components and $N_c$ is the total number of components:

$$\bar{\rho} = \sum_{i=A,B,C,\ldots}^{N_C} \tilde{\rho}_i \tag{1}$$

Mass fraction of component i is given by

$$Y_i = \frac{\tilde{\rho}_i}{\bar{\rho}} \tag{2}$$

$$\sum_{i=A,B,C,\ldots}^{N_c} Y_i = 1$$

An arbitrary constitutive fluid property α ( is defined in the following relation:

$$\alpha = \sum_{i=A,B,C,\ldots}^{N_c} Y_i \cdot \alpha_i \tag{3}$$

Mass-average velocity of component i is presented by $\tilde{u}_{ij}$, and mass-average velocity field is defined in Eq. 4:

$$\tilde{U}_j = \frac{1}{\bar{\rho}} \sum \left( \tilde{\rho}_i \cdot \tilde{U}_{ij} \right) \tag{4}$$

### Transport Equations for Components

The transport equation for each component is given by Eq. 5:

$$\frac{\partial}{\partial t}\left(\bar{\rho} \cdot Y_i\right) + \frac{\partial}{\partial x_j}\left(\bar{\rho} \cdot \tilde{U}_j \cdot Y_i\right) = \frac{\partial}{\partial x_j}\left[\Gamma \frac{\partial Y_i}{\partial_{xj}}\right] + S_i \tag{5}$$

The first term on the right-hand side accounts for the mass flux owing to concentration gradients and is ignored in this analysis. The second term, on the right-hand side of equation 5, models chemical reactions.

The chemical reaction in the present case results in the conversion of cellulose into glucose and degradation of glucose to decomposed products. In 1945, Saeman *(8)* presented a kinetic model of wood hydrolysis that is still widely used today. Based on experimental observations, it states that cellulose is hydrolyzed to glucose, which is then degraded. Both of these reactions working in series are modeled as first-order reactions. The reaction rate constants have Arrhenius temperature dependencies, and it is common to modify the Arrhenius expression to include the contribution of acid concentration as well. This is shown in the following relations:

$$C \xrightarrow{k_1} G \xrightarrow{k_2} D \tag{6}$$

$$k_1 = k_{10} \cdot A^{n_1} \cdot e^{-E_1/R \cdot T} \tag{7}$$

$$k_2 = k_{20} \cdot A^{n_2} \cdot e^{-E_2/R \cdot T} \tag{8}$$

In the Eqs. 6–8, $k_1$ and $k_2$ are reaction constants, $A$ is the acid concentration, $E_i$ is the activation energy, and $R$ is the ideal gas constant. The value for the constants is taken from the work of Lee *(4)*, which is a much more recent work in comparison with ref. *8*.

Equations 9, 10, and 11 are transport equations for cellulose, glucose, and decomposed products:

$$\frac{\partial}{\partial t}\left(\bar{\rho}\cdot Y_C\right)+\frac{\partial}{\partial x_j}\left(\bar{\rho}\cdot\tilde{U}_j\cdot Y_C\right)=-k_1\cdot\bar{g}\cdot Y_C \tag{9}$$

$$\frac{\partial}{\partial t}\left(\bar{\rho}\cdot Y_G\right)+\frac{\partial}{\partial x_j}\left(\bar{\rho}\cdot\tilde{U}_j\cdot Y_G\right)=k_1\cdot\bar{\rho}\cdot Y_C-k_2\cdot\bar{\rho}\cdot Y_G \tag{10}$$

$$\frac{\partial}{\partial t}\left(\bar{\rho}\cdot Y_D\right)+\frac{\partial}{\partial x_j}\left(\bar{\rho}\cdot\tilde{U}_j\cdot Y_D\right)=k_1\cdot\bar{g}-k_2\cdot\bar{g}\cdot Y_G\cdot Y_C \tag{11}$$

According to ref. *4*, from which the input parameters are taken, the mass contains 67.2% glucan and 32.8% lignin and other materials. It is assumed that along with the hydrolysis of cellulose, 42.3% of the remaining lignin and other solids is solubilized. We use the letter $L$ to denote these materials and set up a transport equation for the mass fraction of the remaining material:

$$\frac{\partial}{\partial t}\left(\bar{\rho}\cdot Y_L\right)+\frac{\partial}{\partial x_j}\left(\bar{\rho}\cdot\tilde{U}_j\cdot Y_L\right)=-k_s\cdot\bar{\rho}\cdot Y_C \tag{12}$$

$$k_s=0.423\times\frac{32.8}{67.2}\times k_1\approx 0.206\cdot k_1$$

We use notation $Y_A$ to refer to the mass fraction of acid, which is transported by the flow without directly taking part in the reaction:

$$\frac{\partial}{\partial t}\left(\bar{\rho}\cdot Y_A\right)+\frac{\partial}{\partial x_j}\left(\bar{\rho}\cdot\tilde{U}_j\cdot Y_A\right)=0 \tag{13}$$

The remaining component is water, whose mass fraction, $Y_w$, is calculated from the following constraint:

$$Y_C+Y_G+Y_D+Y_L+Y_A+Y_W=1 \tag{14}$$

### *Momentum Equation*

The equation of motion for the fluid is given by the Navier-Stokes equation:

$$\frac{\partial\bar{\rho}\cdot\tilde{U}_j}{\partial t}+\tilde{U}_k\cdot\frac{\partial\bar{\rho}\cdot\tilde{U}_j}{\partial x_k}=-\frac{\partial p}{\partial x_j}+\frac{\partial}{\partial x_k}\left[\eta\left(\frac{\partial\tilde{U}_j}{\partial x_k}+\frac{\partial\tilde{U}_k}{\partial x_j}\right)\right]+S_{Mj} \tag{15}$$

in which $p$ is the fluid pressure, $\eta$ is the dynamic viscosity, and the source term $S_{Mj}$ models body forces. The inertial forces on the left-hand side of the momentum equation balance pressure, internal friction, and external forces. The second term on the right-hand side expresses momentum transfer from points where the velocity is large to points where it is small. Viscosity is then a measure of the resistance of the fluid to this type of momentum transfer and is a material property. When a large number of particles is suspended in a fluid, and the particle size is much smaller than the characteristic length of the flow, the suspension may be treated as a homogeneous medium with an effective viscosity different from the viscosity of the suspending fluid.

The rheology of the particle suspension plays an important role in the hydrolysis process in a flow-through reactor, because it affects the velocity field and thereby the chemical reaction and the distribution of the mass fractions of the components. Hence, the use of this mathematical model in the prediction of the conversion rate requires that the parameters in the viscosity model be determined by experiment.

The viscosity of a particle suspension is affected by the shape and concentration of particles. The viscosity of particle suspensions is usually flow dependent and is often described as a function of the flow shear rate, $\dot{\gamma}$ , *(9–12)*. A common approach to describe suspension viscosity is to model it as a power-law function of the shear rate in the following way:

$$\eta = k \cdot \dot{\gamma}^{\,n-1} \tag{16}$$

When parameter $n$ is greater than 1, the viscosity increases with the shear rate and the suspension flow is shear thickening. When $n$ is less than 1, the opposite situation occurs and the behavior of the flow is shear thinning. In the theoretical studies reported in Raiskinmäki et al. *(12)*, in which both spherical and nonspherical particles were considered, it was shown that shear-thickening behavior appeared at high shear rates and that the phenomenon was particularly profound for particles of irregular shapes. For corn stover suspensions of an average fiber length of 120 μm, shear-thinning behavior has been observed (*see* refs. *9* and *10*). Pimenova and Hanley *(10)* experimentally studied the effect of concentration, and for flocculated suspensions, Gustavsson and Oppelstrup *(11)* assumed a viscosity model in which the effect of the volume fraction of the particles is incorporated.

### Boundary Conditions

The velocities and mass fractions at the flow inlets are given in Table 2 and here:

| | |
|---|---|
| Acid inlet velocity | $U_{in} = 3 \times 10^{-3}$ m/s |
| Acid mass fraction | $Y_A = 0.064$ |

| | |
|---|---|
| Pulp inlet velocity | $V_{in} = 2.5 \times 10^{-3}$ m/s |
| Glucan mass fraction | $Y_C = 0.1344$ |
| Lignin mass fraction | $Y_A = 0.0656$ |

The normal velocity of the mixture flow is set to zero on solid walls.

### Numerical Solution of Equations

To solve the governing equations, a commercially available fluid mechanic solver called CFX was used *(13)*. CFX uses a finite volume method to solve the equations. It uses an iterative method, solving the momentum equations first, and then the equations for the mass fractions. A second-order discretization was set to avoid numerical diffusion. The convergence criterion was chosen so that the imbalances were practically negligible.

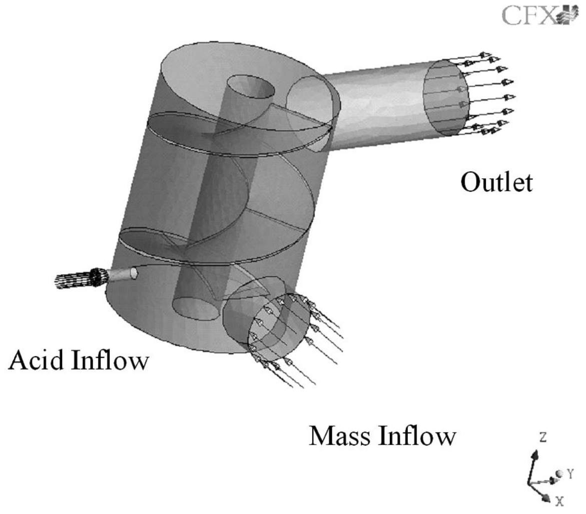

Fig. 1. Simple setup for modeling hydrolysis process in space between two consecutive screw blades.

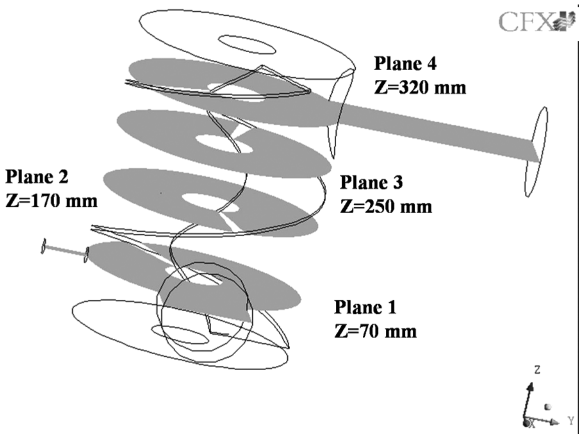

Fig. 2. Sections at which numerical solution is presented.

## Results and Discussion

Figure 1 represents the geometry of the static mixer that is used to test the model. Figure 2 shows the sections in the reactor at which the numerical solutions are presented.

Table 1 gives the parameters associated with the geometry. The geometry and the mesh are built using Ansys software. For solving the equations, CFX fluid mechanics solver is used. Table 2 summarizes input parameters. The kinetic parameters in Table 2 are taken from the work of Lee et al. *(4)*, in which it is stated that these are valid in a temperature range

Table 1
Parameters Associated With Reactor Geometry

| Parameter | Measure |
|---|---|
| Outer diameter | 286 mm |
| Inner diameter | 76.2 mm |
| Length | 400 mm |
| Pulp inlet diameter | 120 mm |
| Pulp outlet diameter | 120 mm |
| Acid inlet diameter | 20 mm |

Table 2
Input Parameters

| Parameter | Expression | Value | Unit |
|---|---|---|---|
| Pulp inlet velocity | $V_{in}$ | $2.5 \times 10^{-3}$ | m/s |
| Acid inlet velocity | $U_{in}$ | $3 \times 10^{-3}$ | m/s |
| Pulp dried mass density | $\rho_{\mathrm{wood}}$ | 1500 | kg/m$^3$ |
| Liquid density | $\rho_1$ | 1000 | kg/m3 |
| Liquid viscosity | $\mu$ | $1. \times 10^{-3}$ | kg/m·s |
| Initial solid mass fraction | — | 0.2 | — |
| Initial glucan mass fraction | $Y_C$ | $0.2 \times 0.675 = 0.1344$ | kg/kg |
| Initial lignin mass fraction | $Y_L$ | $0.2 \times 0.328 = 0.0656$ | kg/kg |
| Initial acid mass fraction | $Y_A$ | 0.064 | kg/kg |
| Acid temperature | $T$ | 478 | $K$ |
| Reaction rate coefficient for glucan | $k_{10}$ | $3.65 \times 10^{17}$ | 1/s |
| Acid concentration exponent | $n_1$ | 1 | — |
| Activity energy for glucan | $E_1$ | 186,358.7 | J/mol |
| Universal gas constant | $R$ | 8.314472 | J K/mol |
| Reaction rate constant for cellulose | $k_1 = k_{10} \cdot A^{n_1} \cdot e^{-E_1/R \cdot T}$ | 0.0001009 | 1/s |
| Reaction rate coefficient for degraded products | $k_{20}$ | $4.72 \times 10^{12}$ | 1/s |
| Acid concentration exponent | $n_2$ | 1 | — |
| Activity energy for glucan | $E_2$ | 139,064.6 | J/mol |
| Reaction rate constant for degraded products | $k_2 = k_{20} \cdot A^{n_2} \cdot e^{-E_2/R \cdot T}$ | 0.000192 | 1/s |
| Percentage of lignin and other materials that are solubilized | | 0.423 | |
| Rate of disappearance of\` lignin and other materials that are solubilized | $k_s$ | $0.423 \times \dfrac{0.328}{0.672} \times k_1$ | 1/s |
| Reynolds number | $\mathrm{Re} = \dfrac{\rho \cdot U \cdot L}{\mu}$ | $\dfrac{1000 \cdot 3 \times 10^{-3} \cdot 0.1}{1. \times 10^{-3}} = 300$ | |
| Froude number | $Fr = \dfrac{U^2}{g \cdot L}$ | $\dfrac{9 \times 10^{-6}}{10 \cdot 0.1} = 9 \times 10^{-6}$ | |

of 205–235°C and with 0.064 wt% sulfuric acid. Here we have assumed that temperature is constant at 205°C, but the acid concentration changes as a result of the flow. Hence, the rate coefficients vary locally with the variation of the acid concentration. The velocities are of the same order of magnitude as those in Lee et al. *(4)*. The reactor is a static mixer and the simulations are performed in steady-state condition. As shown in Table 2, Reynolds number, based on the distance between the reactor wall and the screw axis, is about 300; hence, the flow is laminar. With gravity in the y-direction, and the same typical distance as in the estimation of Reynolds number, the Froude number and, for this reason, the gravitational effects become very small.

Figure 3 shows the acid mass fraction/concentration at different planes. Darker areas correspond to where the acid concentration is high. The highest acid concentration is, obviously, in the acid inflow pipe, as shown in plane 1 in Fig. 3. A large region of plane 1 is not yet affected by the acid, but as the mass and the acid flow along the blades, more acid comes into contact with the mass and chemical reaction takes place. As a result of the hydrolysis process and dissolution of the solid phase, the mass fraction of the liquid phase increases and the acid will become more dilute. For instance, in plane 4 in Fig. 3, one can see that the highest value of the acid mass fraction is about 0.0026, which is lower than the initial value of 0.064 at the acid inflow pipe in plane 1. As a result of the dilution of acid, the reaction rate decreases, as shown in Eqs.7 and 8. It should be mentioned that in the earlier studies *(4)* and *(5)*, the acid concentration is assumed constant and, therefore, the reaction rates are constant. Such an assumption results in an overestimation of the conversion rate.

Figure 4 depicts glucan mass fractions at different planes. As in Fig. 3, the darker areas are related to regions of a higher level of mass fraction. As can be seen in Fig. 4, the presence of the acid results in the conversion of glucan. A quantitative measure of the degree of the conversion is given by comparing the averaged value of the mass fraction of the glucan at the outlet with the corresponding value at the mass inlet. The percentage of the converted glucan in this case is about 6.6%, and the mass of the produced glucose was 0.022 kg. Figure 4 gives an idea as to what degree the glucan is converted after the pulp has flowed along about one and half screw blades. The size of the reactor and the number of screw blades in a plant are of course much larger. As a result, the acid and the pulp will be better mixed and a larger proportion of glucan will be converted in a plant-sized reactor.

## Conclusion

We have presented a mathematical model to describe both the flow and chemical reaction during the dilute-acid hydrolysis of cellulose particles. The model considers the particles and the surrounding liquid as a single continuum phase consisting of several components. The material properties of this phase then become weighted averages of the material properties of its constituents. In this description, the particle-particle and

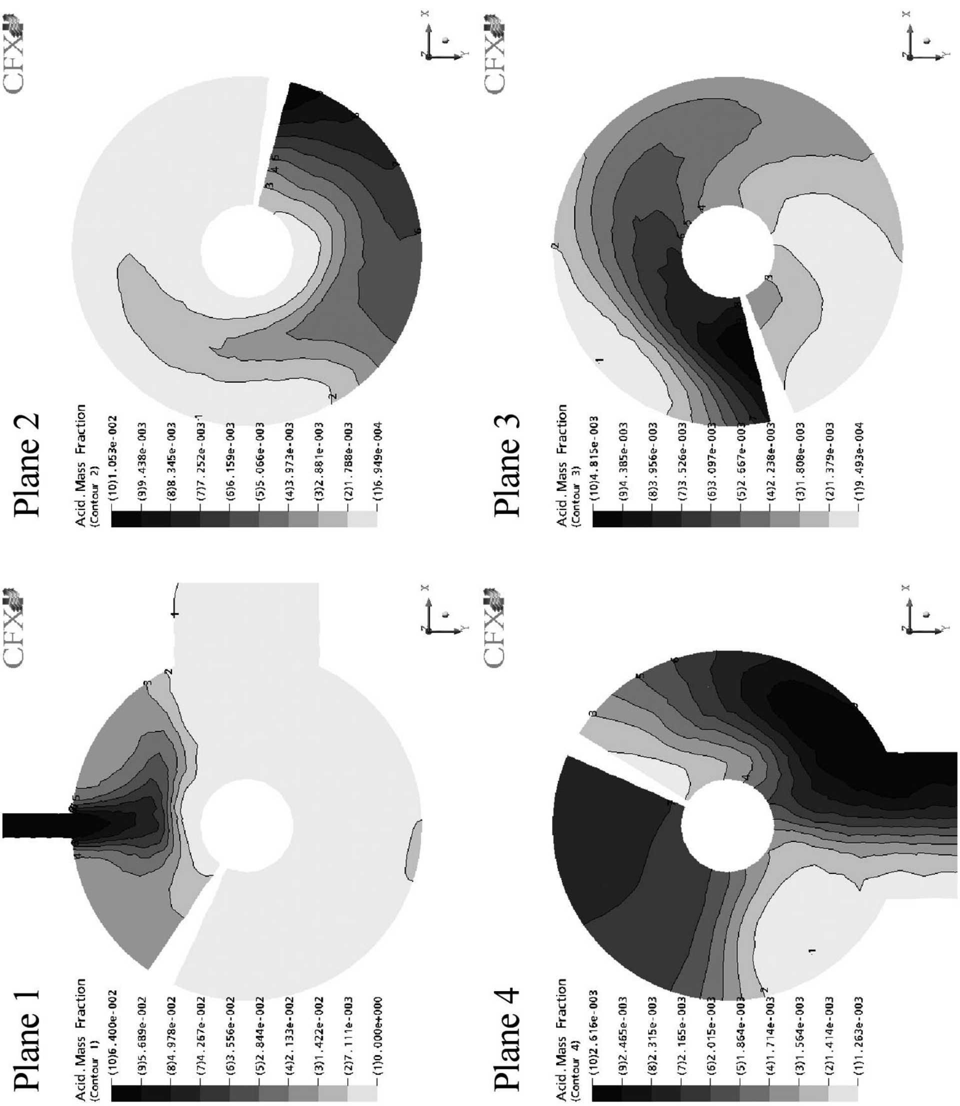

Fig. 3. Mass fraction of acid at different sections; darker areas represent higher values.

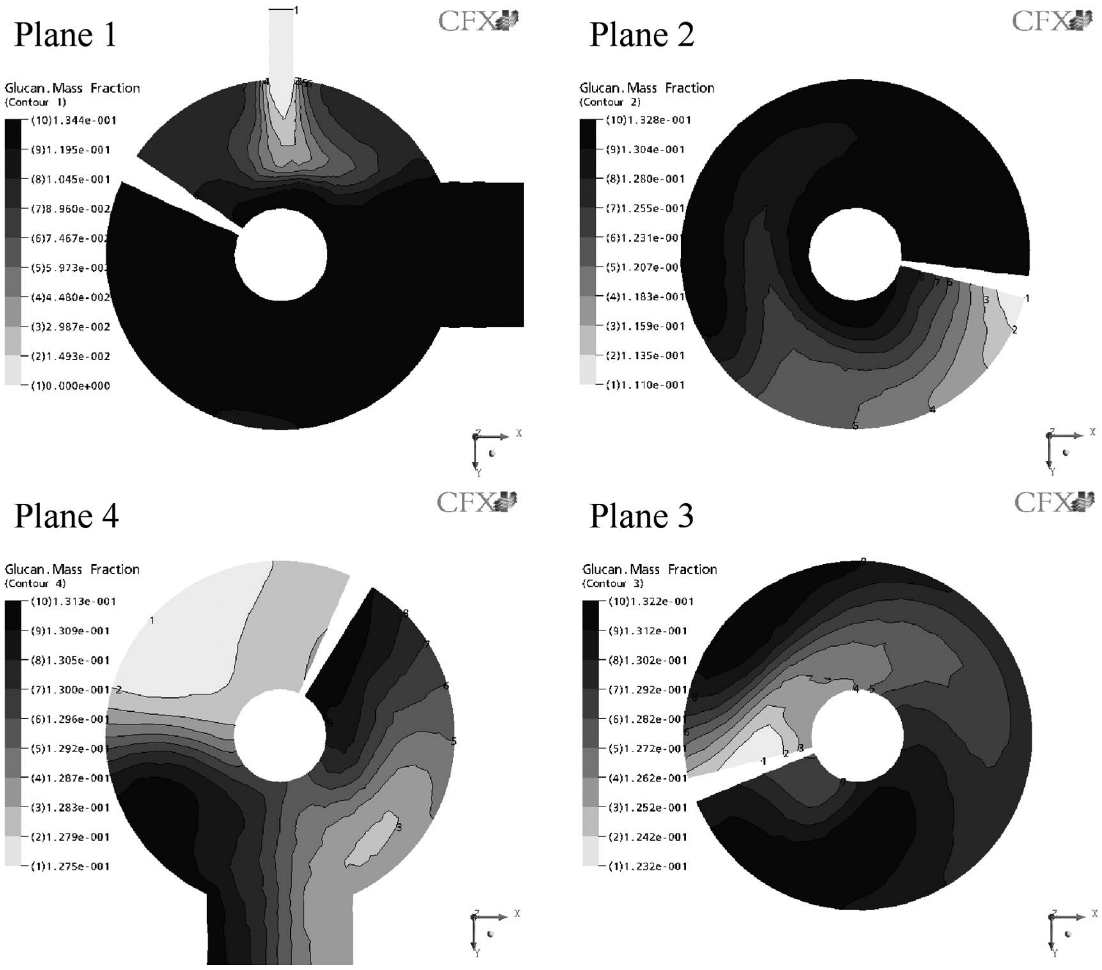

Fig. 4. Mass fraction of glucan at different sections; darker areas represent higher values.

particle-liquid interactions have to be described in the viscosity model. There is evidence in the literature that the viscosity of particle suspensions can be described as a power-law function of the shear rate. Such a model has two parameters, which should be determined by experiments.

The model was used to simulate the dilute-acid hydrolysis process of cellulose particles in a static mixer, in which the mass and the acid enter into the reactor, then leave it after flowing about two turns around the screw blades. Literature data were used for input parameters, and constant viscosity was assumed for this test. In contrast to previous studies, we did not assume constant reaction rates. The reaction rates are proportional to the acid mass fraction, for which we solve a transport equation. As a result, the reaction rate is not uniform and reaction takes place only in the presence of the acid. The simulation result can be presented in terms of velocity and mass fraction of components at any position in the computation domain. Thus, if the model is applied to the conditions that occur in a plant and the geometry of a reactor, then the simulation results can be used to predict the conversion rate of glucan to sugar.

Because screw conveyers are also used in plant reactors, it is reasonable to use a viscosity model to describe the shear forces, which are significant in the flow of the mass between the blades. In the flow entrance region of the reactor, the difference in velocity between the acid and the mass is high, which causes momentum transfer between the two flows. Therefore, a two-phase flow model is probably more suitable to account for such effects. Such a model will be presented in another article.

One advantage of the present model is that single-phase, multicomponent flow requires four momentum equations to be solved, as opposed to seven for the two-phase flow. Moreover, only two material parameters need to be determined. As a result, it is a practical choice for use in plants to optimize and determine those operational parameters that predict highest glucose production.

## Acknowledgments

We wish to thank the staff of Etek for additional support, and for providing a stimulating working environment. We also gratefully acknowledge financial support granted by the Swedish Foundation for Strategic Environmental Research (Mistra).

## References

1. Mielenz, J. R. (2001), *Curr. Opin. Microbiol.* 4, 324–329.
2. Target, R. and Elander R., report number/BR-420-21221 4/97, National Renewable Energy Laboratory, 1997.
3. Nguyen, Q. A., Dickow, J. H., Duff, B. W., et al.(1996), *Bioresour. Technol.* **58,** 189–196.
4. Lee, Y. Y., Wu, Z., and Torget, R. W. (2000), *Bioresour. Technol.* **71,** 29–39.
5. Pettersson, P. O., Eklund, R., and Zacchi, G. Proceedings I:7, International Symposium on Alcohol Fuels XIII, July 3–6, 2002, Stockholm, Sweden.

6. Wan, Y. and Hanley, T. R. (2003), *Appl. Biochem. Biotechnol.* **105–108,** 593–602.
7. Wan, Y. and Hanley, T. R. (2004), *Appl. Biochem. Biotechnol.* **113–116,** 733–745.
8. Saeman, J. F. (1945), *Ind. Eng. Chem.* **37,** 43–52.
9. Pimenova, N. V. and Hanley, T. R. (2003), *Appl. Biochem. Biotechnol.* **105–108,** 383–392.
10. Pimenova, N. V. and Hanley, T. R. (2004), *Appl. Biochem. Biotechnol.* **113–116,** 347–360.
11. Gustavsson, K. and Oppelstrup, J. (2001), *J. Eng. Math.* **41,** 189–201.
12. Raiskinmäki, P., Shakib-Manesh, A., Koponen, A., Kataja, M., and Timonen, J. (2000), *Comput. Phys. Commun.* **129,** 185–195.
13. Ansys Company, CFX-5.7 Solver Theory Manual, CFX Ltd. Oxfordshire, 2004, pp. 26–30.